Indian J Phys (August 2023) 97(9):2685–2692
https://doi.org/10.1007/s12648-023-02614-1

ORIGINAL PAPER

First-principles study on structural, electronic, and elastic properties of SrFCl

Y Güzel[1], H Öztürk[2]*, C Kürkçü[3] and Ç Yamçıçıer[4]

[1]Institute of Science, Kırşehir Ahi Evran University, Kırşehir, Turkey

[2]Department of Physics, Kırşehir Ahi Evran University, Kırşehir, Turkey

[3]Department of Electronics and Automation, Kırşehir Ahi Evran University, Kırşehir, Turkey

[4]Department of Electricity and Energy, Osmaniye Korkut Ata University, Osmaniye, Turkey

Received: 04 August 2022 / Accepted: 22 January 2023 / Published online: 15 February 2023

Abstract: Structural, electronic, and elastic properties of SrFCl, one of the alkaline-earth fluorohalides, under high pressure were investigated using the Siesta Package Program within the framework of density functional theory. SrFCl crystallizes in a tetragonal matlockite type structure belonging to the space group P_4/nmm at ambient conditions. The phase transformation from a tetragonal matlockite type structure to an orthorhombic type structure belonging to the space group *Pmmn* occurred in the presence of gradually increasing simulation pressure. The values of lattice parameters, shear modulus, Young's modulus, and bulk modulus, for the obtained structures of SrFCl were investigated. The transition pressure value was calculated by total energy and enthalpy calculations. The electronic properties of SrFCl were also calculated. Band gaps of 6.52 eV for the P_4/nmm phase and 3.55 eV for the *Pmmn* phase were obtained. Thus, it was concluded that the P_4/nmm and *Pmmn* phases of SrFCl have an insulator and a semiconductor character, respectively. In addition to these studies, the mechanical stability of SrFCl was investigated by calculating elastic constants. As a result of this calculation, both phases of SrFCl were mechanically stable.

Keywords: Ab-initio calculation; Enthalpy; Phase transition; Electronic and elastic properties

1. Introduction

SrFCl, one of the matlockite-type PbFCl families, crystallizes in a tetragonal layered structure corresponding to the space group P_4/nmm under ambient conditions [1–7]. In this structure, there are two SrFCl molecules per unit cell. Sr atoms are located in 2c (1/4, 1/4, z) Wyckoff positions, $z = 0.2974$. F atoms are located in 2b (3/4, 1/4, 1/2) Wyckoff positions. Cl atoms are located in 2c (1/4, 1/4, z) Wyckoff positions, $z = 0.8512$. Under high pressure, SrFCl undergoes a structural phase transition and transforms into an orthorhombic structure belonging to the space group *Pmmn*. In both the P_4/nmm and *Pmmn* phases, SrFCl has 6 atoms in the unit cell. In an orthorhombic structure, Sr atoms are located in 2a (1/4, 1/4, z) Wyckoff positions, $z = 0.2824$. F atoms are located in 2b (1/4, 3/4, z) Wyckoff positions, $z = 0.4478$. Cl atoms are located in 2a (1/4, 1/4, z) Wyckoff positions, $z = 0.8913$.

The properties of alkaline-earth fluorohalides *MFX* (M = Sr, Ba, Ca, Pb; X = Cl, Br, I) form an important class of materials that have been extensively investigated because they have practical applications such as medical imaging, as a sensor in diamond anvil cells at high temperature, photoconductivity, photoluminescence, and anisotropic ionic conductivity [8–16]. Besides, some dihalides such as BaFCl and BaFBr are used in spectroscopic and nuclear detectors [17].

In addition, these compounds have been used in many theoretical and experimental studies due to their layered structure in the last quarter century [11, 18–21]. Öztürk et al. [20] calculated the structural, electronic, and elastic properties of SrFI using the ab-initio method. Liu et al. [22] studied the electronic, optical, and luminescent properties of the P_4/nmm phase of PbFCl using the plane waves and pseudopotential method. Kanchana et al. [23], using the self-consistent tight-binding linear muffin-tin orbital

*Corresponding author, E-mail: hozturk@ahievran.edu.tr

method (TB-LMTO), calculated the structural and electronic properties of SrFI, SrFBr, and CaFBr. Besides, Hassan et al. [24], using the full-potential linear augmented plane wave method (FP-LAPW), theoretically studied the electronic properties of *MFX* (*M* = Sr, Ba, Pb; *X* = Cl, Br, I). Unfortunately, there is no study in the literature on the new phase (*Pmmn*) of these compounds obtained under high pressure. Therefore, for the tetragonal and orthorhombic structure of SrFCl, the structural, electronic, and elastic properties under high pressure were also examined. Thanks to the new structure obtained in this study, it is thought that it will lead to experimental studies.

In this paper, the calculations are performed using the ab-initio method in the framework of the density functional theory (DFT), and the paper is organized as follows. In Sect. 2, the calculation methods used in this study are given. Results and discussion are given in Sect. 3 and the conclusions in Sect. 4.

2. Methods

In this study, the phase transformation mechanism that occurs in the structure of SrFCl compound under high pressure was studied with the Siesta Package Program [25] within the framework of density functional theory (DFT). DFT calculations used the Perdew–Burke–Ernzerhof (PBE) [26] parameterization of the generalized gradient approximation to the exchange–correlation energy. We used Troullier–Martins [27]-type norm-conserving pseudopotentials for Sr, F, and Cl atoms. The double-ζ polarization (DZP) basis set was used, which has given much better results in the simulations. Using the periodic boundary conditions, the unit cell consisting of 6 atoms was increased to 108 atoms by applying a 3 × 3 × 2 supercell. The optimization of volume of this supercell with 108 atoms and the atomic structure obtained at each pressure value were managed using the Parrinello–Rahman technique [28]. Monkhorst–Pack mesh [29] was used 8 × 8 × 5 and 8 × 6 × 3 for tetragonal and orthorhombic structures of SrFCl, respectively. Simulation pressure was applied in increments of 10 GPa pressure. The crystal structures of SrFCl were analyzed using the KPlot Program [30] and RGS algorithms [31]. In this way, we were able to have detailed information about the lattice parameters, atomic positions, and space groups of the analyzed structure.

3. Results and discussions

3.1. Structural properties

In this study, the structure of the matlockite-type SrFCl compound was investigated under 0 GPa pressure. The lattice parameters were obtained as $a = b = 4.0719$ Å and $c = 6.6644$ Å. There are 6 atoms in the unit cell of the tetragonal structure of SrFCl. Increasing pressures in increments of 10 GPa were applied to this structure up to 250 GPa. The phase transition from P_4/nmm phase to the *Pmmn* phase was obtained at a simulation pressure of 190 GPa. The lattice parameters of this *Pmmn* phase were obtained as $a = 2.6228$ Å, $b = 3.7028$ Å, and $c = 6.3659$ Å. An image of the crystal structures of the phases obtained for SrFCl is given in Fig. 1.

In the next step, the change in volume versus pressure is examined to obtain information about the phase transformation and is given in Fig. 2. It was observed that the volume values decreased with increasing pressure. When the pressure reached 190 GPa, there was a sharp decrease in the volume value. This discontinuity is proof that the phase transformation is in the first order.

The transition pressure values obtained during the phase transformations under the influence of the simulation pressures applied to the systems are usually higher than the experimental results. The differences in these transition pressures are due to some simulation conditions. While the crystal structures of real compounds are not perfect, in simulation studies, it is accepted that the crystal is perfect, that is, without defects, despite boundary conditions and surface defects. In addition, in simulation studies, the system is faced with an energy barrier and is exposed to excessive pressure to cross this barrier [32]. On the contrary, the transition pressure value obtained from the enthalpy result is in good agreement with the experimental results. Therefore, in the next step, total energy–volume and pressure–enthalpy relationships were examined.

Energy–volume calculations were made to find out which phases obtained for SrFCl are more stable. The energy–volume curves are given in Fig. 3.

The unit cells of obtained structures for SrFCl were used in this calculation. In addition, the energy and volume values were fitted to the 3rd-degree Birch–Murnaghan equation of state [33, 34] as given in Eq. 1.

$$E = E_0 + \frac{9V_0B_0}{16}\left\{\left[\left(\frac{V_0}{V}\right)^{\frac{2}{3}} - 1\right]^3 B_0{}' + \left[\left(\frac{V_0}{V}\right)^{\frac{2}{3}} - 1\right]^2 \left[6 - 4\left(\frac{V_0}{V}\right)^{\frac{2}{3}}\right]\right\} \tag{1}$$

In Eq. 1, E_0, V_0, $B_{0,}$ and $B_0^{'}$ are energy, volume, bulk modulus, and pressure derivative of the bulk modulus at ambient pressure, respectively. At the same time, using Eq. 2, we can also calculate the external pressure applied to the system.

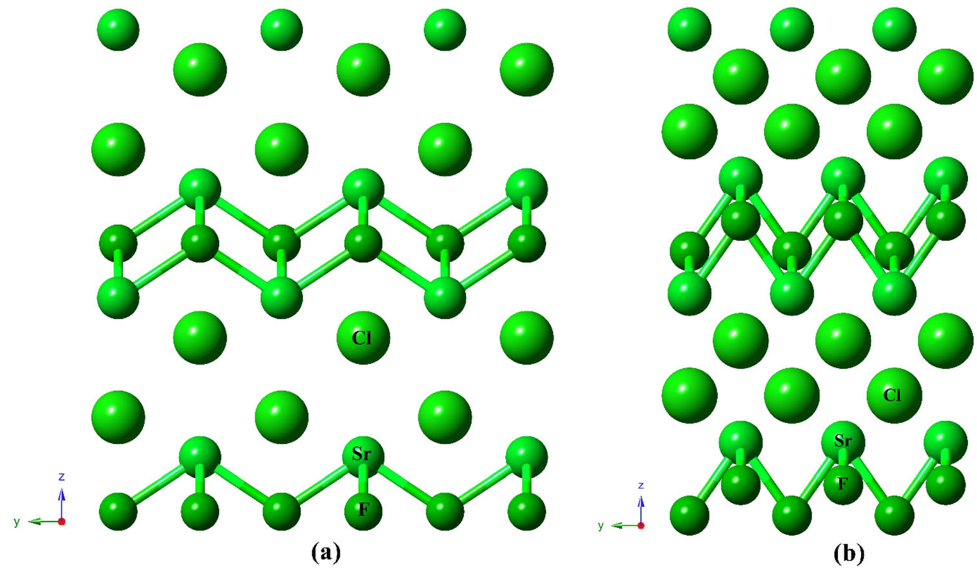

Fig. 1 Supercell structures of stable phases of SrFCl: (**a**) P_4/nmm, (**b**) $Pmmn$

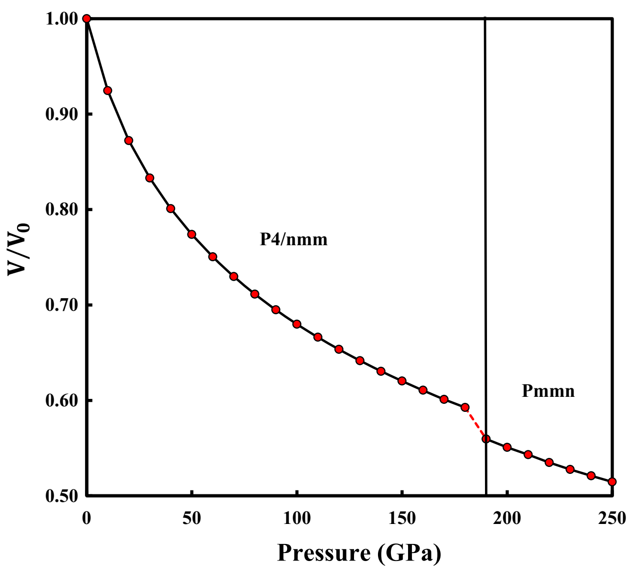

Fig. 2 Graph of change in volume value as a function of pressure

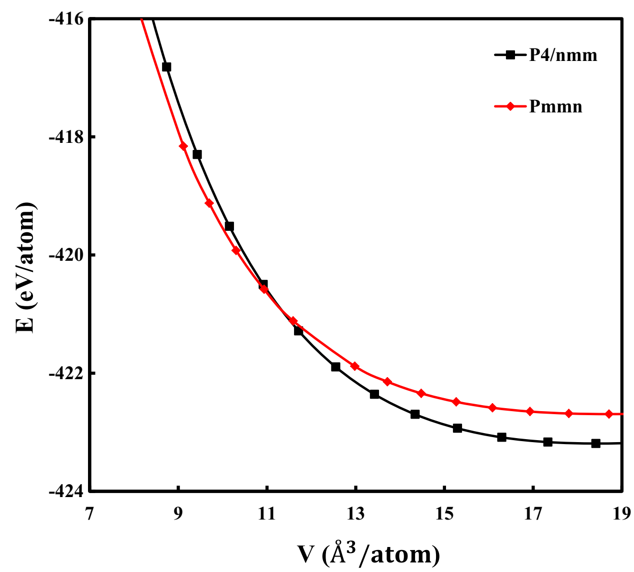

Fig. 3 Graph of change in volume value as a function of energy

$$P = \frac{3}{2}B_0\left[\left(\frac{V_0}{V}\right)^{7/3} - \left(\frac{V_0}{V}\right)^{5/3}\right] \times \left\{1 + \frac{3}{4}(B_0^{'} - 4)\left[\left(\frac{V_0}{V}\right)^{2/3} - 1\right]\right\} \quad (2)$$

The pressure value given in Eq. 2 is found by $P = -\left[\frac{\partial E}{\partial V}\right]_{T=0K}$.

As shown in Fig. 3, P_4/nmm phase with minimum energy for SrFCl is more stable. Equilibrium lattice parameters and volume values obtained from this study with previous experimental and theoretical studies are summarized in Table 1.

Enthalpy calculations usually give transition pressure values close to experimental data. The intersection point of the enthalpy curves obtained for both phases of SrFCl gives the phase transition pressure value. The enthalpy curves obtained against pressure for SrFCl are given in Fig. 4. According to this figure, the phase transition pressure value from P_4/nmm phase to the $Pmmn$ phase was obtained as 140 GPa.

3.2. Elastic properties

It is very important to know the second-order independent elastic constants (C_{ij}) under the applied stress/strain, which give information about the hardness and

Table 1 The calculated transition pressure (P_t), lattice parameter (a, b, c), and volume (V) values for the obtained structures of SrFCl

Phases	P_t (GPa)	a (Å)	b (Å)	c (Å)	V (Å)	References
P_4/nmm	0	4.0719	4.0719	6.6644	110.50	This study
		4.1259	4.1259	6.9579	118.45	[42]
		4.185	4.185	7.057	123.60	[24]
		4.176	4.176	6.990	121.90	[43]
		4.126	4.126	6.958	118.50	[40]
		4.129	4.129	6.966	118.76	[44]
Pmmn	148	2.6228	3.7028	6.3659	61.82	This study

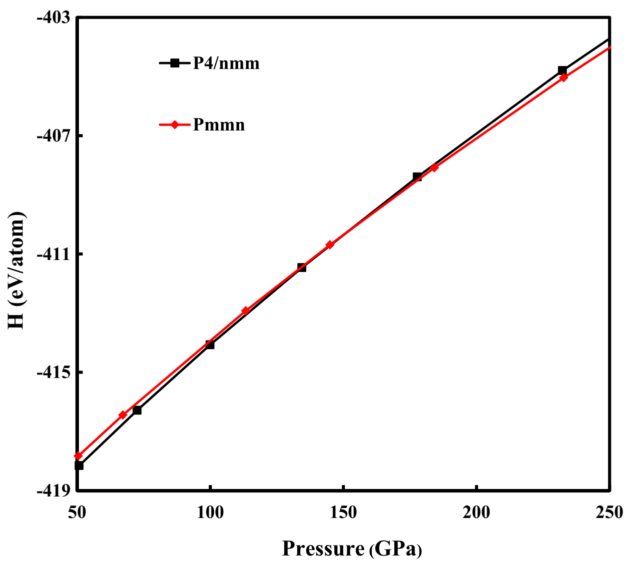

Fig. 4 Graph of enthalpy as a function of pressure

mechanical stability of the materials. In Table 2, the values of the elastic constants for the P_4/nmm and *Pmmn* phases are given.

The number of second-order independent elastic constant values obtained for the tetragonal and orthorhombic type structures of SrFCl is six ($C_{11}, C_{12}, C_{13}, C_{33}, C_{44}, \text{and}\, C_{66}$) [35] and nine ($C_{11}, C_{22}, C_{33}, C_{44}, C_{55}, C_{66}, C_{12}, C_{13}, \text{and}\, C_{23}$) [36–38], respectively.

The stability criteria of Born, well known in the literature, for the tetragonal structure, are given below:

$$C_{11} > 0, C_{33} > 0, C_{44} > 0, C_{66} > 0, (C_{11} - C_{22}) > 0, (C_{11} + C_{33} - 2C_{13}) > 0, (2C_{11} + C_{33} + 2C_{12} + 4C_{13}) > 0 \tag{3}$$

The stability criteria of Born for orthorhombic structure are as follows:

$$C_{11} > 0, C_{22} > 0, C_{33} > 0, C_{44} > 0, C_{55} > 0, C_{66} > 0, C_{11}C_{22}C_{33} + 2C_{12}C_{13}C_{23} - C_{11}C_{23}^2 - C_{22}C_{13}^2 - C_{33}C_{12}^2 > 0, C_{11}C_{22} > C_{12}^2 \tag{4}$$

The Born criteria give information about whether the material is mechanically stable or not [38]. In this study, both structures are mechanically stable. The data of some parameters related to the durability of the material are given in Table 3. These data are calculated using 2nd-order elastic constant values.

Using the second-order elastic constant values, we calculated the bulk modulus (B), which expresses the resistance corresponding to volume change in the presence of pressure. With the increase in volume, the resistance of the material changes in direct proportion. It is a representation

Table 3 The calculated bulk modulus B (GPa), shear modulus G (GPa), G / B and B / G ratios, Poisson's ratios σ, and Young's modulus E (GPa) values for SrFCl

Phases	B	G	G/B	B/G	σ	E
P_4/nmm	69.80	30.45	0.44	2.29	0.310	79.6
Pmmn	462.60	145.12	0.31	3.18	0.358	394.22

Table 2 The calculated independent elastic constant values C_{ij} (GPa) for the obtained structures of SrFCl

Phases	C_{11}	C_{12}	C_{13}	C_{22}	C_{23}	C_{33}	C_{44}	C_{55}	C_{66}
P_4/nmm	80.87	19.05	23.37	–	–	30.65	23.42	–	26.69
Pmmn	439.28	201.81	372.86	567.42	319.16	578.20	8.77	165.99	273.90

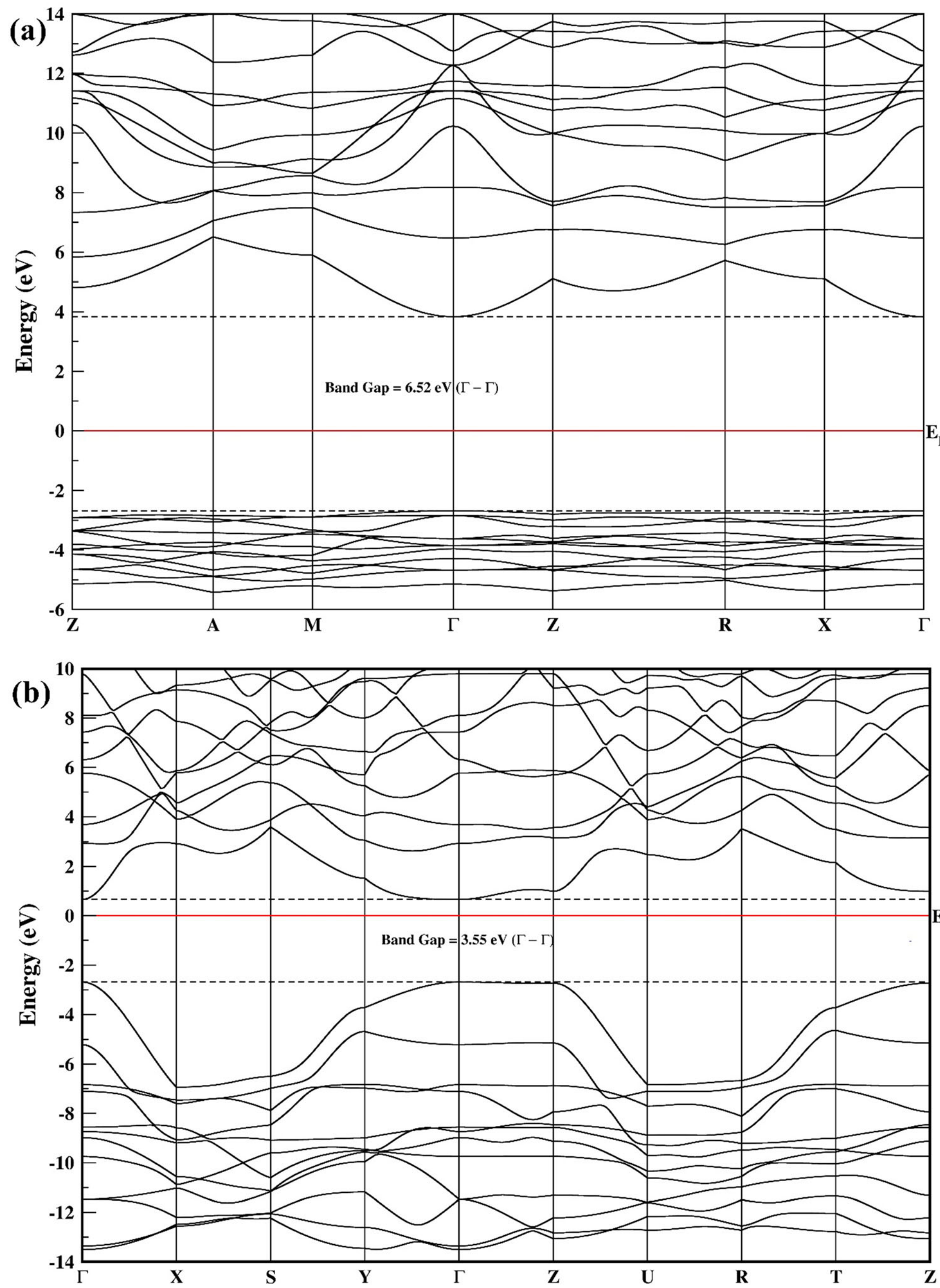

Fig. 5 Electronic band distribution curves corresponding to high symmetry points: (**a**) P_4/nmm, (**b**) *Pmmn*

of the hardness of materials and is a measure of the energy required for the resistance of the material to change in volume under high pressure.

Then, using the elastic constant values, we calculated the shear modulus (*G*), which expresses the resistance corresponding to the shape change in the presence of pressure. It is one of the most important parameters that determine the hardness measure, and the hardness of a material is a measure of the resistance of that material to the stress of another material on its surface. As shown in Table 3, the obtained orthorhombic *Pmmn* phase of SrFCl has a higher *G* value than the tetragonal P_4/nmm phase. Therefore, it is understood that the orthorhombic structure of SrFCl has higher hardness than the tetragonal-type structure. Thus, shear modulus and bulk modulus results to support each other. Information about the brittleness and ductility of materials can be estimated by looking at the *B*/*G* ratio. This ratio is defined by Pugh [39] and the limit value is taken as 1.75. If the *B*/*G* ratio obtained for the phases of SrFCl is above 1.75, it is ductile, otherwise, it is brittle. SrFCl, whose *B*/*G* ratio obtained for both phases in this study are greater than 1.75, has ductile properties in these phases.

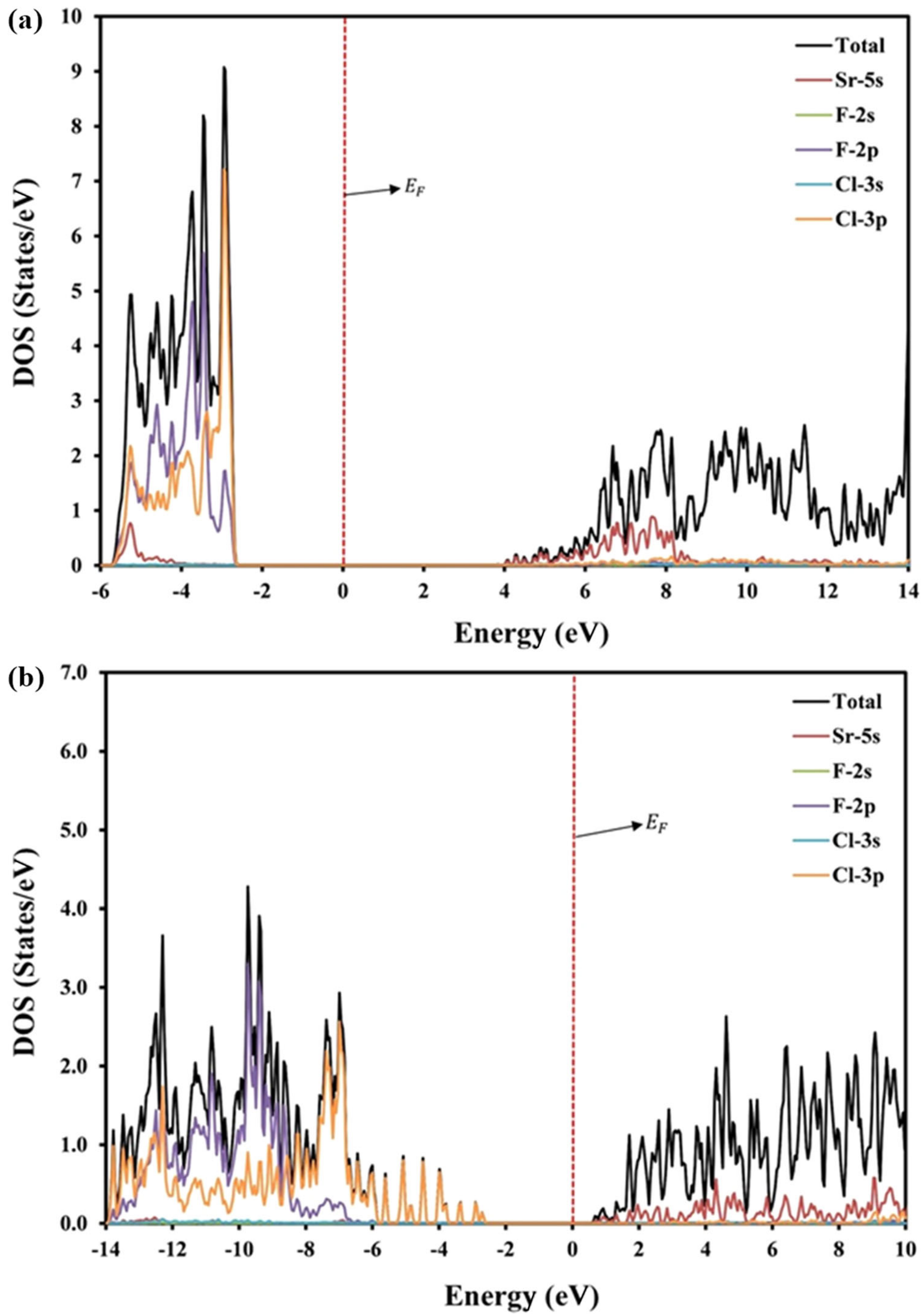

Fig. 6 Density of states curves as a function of energy: (**a**) P_4/nmm, (**b**) *Pmmn*

The next parameter, the Poisson's ratio (σ), gives information about the bonding (covalent bonding) properties of the materials and is given as follows:

$$\sigma = \left(\frac{3B - E}{6B}\right)$$

The higher the Poisson's ratio, the higher the plasticity property of the materials. If this ratio is around 0.1, the material has made covalent bonds in that phase. If this ratio is around 0.25, it is said to have made an ionic bond. Poisson's ratio value given in Table 3 was obtained as 0.310 for P_4/nmm of SrFCl at 0 GPa pressure. Therefore, the ionic character of SrFCl is more dominant in this phase. Under high pressure, the Poisson's ratio value for the *Pmmn* phase of SrFCl was obtained as 0.358. In this phase, as in P_4/nmm, the ionic character is more dominant. Thus, SrFCl has ionic bonds in both phases.

The last parameter, Young's modulus (E), corresponds to the hardness of the material. From the calculated values of the bulk Modulus and Poisson's ratio, the stress/strain ratio that occurs when a tensile or compressive force is applied to the material is defined as Young's modulus.

It is seen that Young's modulus value increases as the pressure applied to the material increases. Thus, the hardness of the material also increases.

3.3. Electronic properties

For both phases obtained at a simulation pressure of 0 GPa and 190 GPa of SrFCl, the electronic band structures were calculated along with the high symmetry directions. Electronic band structure graphs calculated for P_4/nmm and *Pmmn* phases are shown in Fig. 5a, b, respectively.

The Fermi energy level was fitted to 0 eV and indicated by a red solid line. The valence band is below the Fermi energy level and the conduction band is above it. These two bands are separated from each other by a bandgap of 6.52 eV for the P_4/nmm phase and 3.55 eV for the *Pmmn* phase. Therefore, the P_4/nmm phase of SrFCl is an insulator, whereas the *Pmmn* phase is a semiconductor. In addition, as the maximum point of the valence band and the minimum point of the conduction band are at the same symmetry point (Γ–Γ), both phases of SrFCl have a direct band transition [40, 41].

To obtain more detailed information about the electronic properties, the density of states curves for both phases of SrFCl were examined and given in Fig. 6a, b, respectively.

The Fermi energy level was set to 0 eV and indicated by the red dashed line. From Fig. 6a, below the Fermi energy level, the largest contribution between (0)–(− 3) eV came from Cl-3*p*, but between (− 3) and (− 6) eV, the largest contribution came from F-2*p*. Above the Fermi energy level, the largest contribution came from Sr-5*s*. In Fig. 6b, the largest contribution between (0) and (− 8) eV below the Fermi energy level came from Cl-3*p*. Similarly, the largest contribution between (− 8) and (− 13) eV came from F-2*p*. Above the Fermi energy level, the largest contribution came from Sr-5*s*.

4. Conclusions

In this work, structural, electronic, and elastic properties of SrFCl have been studied with the effect of pressure using ab-initio calculations. The simulation studies show two different structures, the space group P_4/nmm and *Pmmn*, for SrFCl. As a result of the literature study, the *Pmmn* phase was suggested for the first time in this study. The P_4/nmm phase of SrFCl has an insulating character because it has a wide band gap of 6.52 eV around the Fermi energy level. In the *Pmmn* phase, on the contrary, it has a semiconductor character because it has a band gap of 3.55 eV between the maximum of the valence band and the minimum of the conduction band around the Fermi energy level. In addition, as the maximum of the valence band and the minimum of the conduction band are at the same symmetry point, it is a direct band-transition semiconductor. The elastic constants of SrFCl were calculated for the 0 GPa and high-pressure phases. The independent elastic constant values obtained were fitted to the well-known Born stability criteria in the literature for tetragonal P_4/nmm and orthorhombic *Pmmn* phases, and both phases obtained for SrFCl were found to be mechanically stable. In addition, the bulk modulus (B) and shear modulus (G), which give information about the hardness of the material, were also calculated. According to the B/G value (more than 1.75), which is the ratio of these two values to each other, SrFCl was found to have ductile properties in both phases. Besides, Poisson's ratio was calculated to predict the bonding between the atoms that compose the material. In both phases of SrFCl, it was observed that the atoms formed ionic bonds with each other.

References

[1] M Barhoumi, N Sfina and M Said *Solid State Commun.* **336** 114430 (2021).
[2] H Ubukata, K Ishida, Y Higo, Y Tange, T Broux, C Tassel and H Kageyama *J. Solid State Chem.* **312** 123253 (2022).
[3] M Barhoumi and M Said *Mater. Chem. Phys.* **252** 123233 (2020).
[4] J Tan, Q Hao, Z Zeng, X Chen and H Geng *J. Phys. Chem. Solids* **153** 109956 (2021).
[5] L Kunduru, N Yedukondalu, S C Rakesh Roshan, S Sripada, M Sainath, L Ehm and J B Parise *J. Phys. Chem. C* **125** 17261 (2021).
[6] A Sabry *Comput. Condens. Matter* **33** e00743 (2022).
[7] Y Sorb and D Sornadurai *Materials Research Bulletin* **65** 1 (2015).
[8] T K Anh, W Strek and C Barthou *J. luminesc.* **72** 745 (1997).
[9] M Secu, L Matei, T Serban and E Apostol *Opt. Mater* **15** 115 (2000).
[10] Y Shen, T Gregorian and W Holzapfel *High Press. Res.* **7** 73 (1991).
[11] F Decremps, M Fischer, A Polian, J Itie and M Sieskind *Phys. Rev. B* **59** 4011 (1999).
[12] J F Scott *J. Chem. Phys.* **49** 2766 (1968).
[13] B Sundarakannan, T Ravindran, R Kesavamoorthy and S Satyanarayana *Solid State Commun.* **124** 385 (2002).
[14] F Decremps, M Gauthier, J C Chervin, M Fischer and A Polian *Phys. Rev. B* **66** 024115 (2002).
[15] D M Adams and T K Tan *Journal of Physics and Chemistry of Solids* **42** 559 (1981).
[16] T Kuzuba, Y Sato, S Yamaoka and K Era *Phys. Rev. B* **18** 4440 (1978).
[17] M Crawford, L Brixner and K Somaiah *J. Appl. Phys.* **66** 3758 (1989).

[18] M Pasero and N Perchiazzi *Mineralogical Magazine* **60** 833 (1996).

[19] F Decremps, M Fischer, A Polian, J Itie and M Sieskind *Eur. Phys. J. B Condens. Matter Complex Syst.* **9** 49 (1999).

[20] H Öztürk, Y Güzel and C Kürkçü *Solid State Commun.* **336** 114399 (2021).

[21] M Canpolat, C Kürkçü, Ç Yamçıçıer and Z Merdan *Solid State Commun.* **288** 33 (2019).

[22] B Liu, C Shi, M Yin, Y Fu and D Shen *J. Phys.: Condens. Matter* **17** 5087 (2005).

[23] V Kanchana, G Vaitheeswaran and M Rajagopalan *J. Phys.: Condens. Matter* **15** 1677 (2003).

[24] F El haj Hassan, H Akbarzadeh, S Hashemifar and A Mokhtari *J. Phys. Chem. Solids* **65** 1871 (2004).

[25] P Ordejón, E Artacho and J M Soler *Phys. Rev. B* **53** R10441 (1996).

[26] J P Perdew, K Burke and M Ernzerhof *Phys. Rev. Lett.* **77** 3865 (1996).

[27] N Troullier and J L Martins *Physical review B* **43** 1993 (1991).

[28] M Parrinello and A Rahman *Physical review letters* **45** 1196 (1980).

[29] H J Monkhorst and J D Pack *Physical review B* **13** 5188 (1976).

[30] R Hundt, J C SchoÈn, A Hannemann and M Jansen *J. Appl. Crystallogr.* **32** 413 (1999).

[31] A Hannemann, R Hundt, J Schön and M Jansen *J. Appl. Crystallogr.* **31** 922 (1998).

[32] H Öztürk and M Durandurdu *J. Am. Ceram, Soc.* **94** 932 (2011).

[33] F Birch *Phys. Rev.* **71** 809 (1947).

[34] F Murnaghan *Proc. Nation. Acad. Sci. USA* **30** 244 (1944).

[35] M Özduran, A Candan, S Akbudak, A Kushwaha and A İyigör *J. Alloys Compd.* **845** 155499 (2020).

[36] C Kurkcu, S Al and C Yamcicier *Chem. Phys.* **539** 110934 (2020).

[37] S Al, C Kurkcu and C Yamcicier *Int. J. Hydrogen Energy* **45** 4720 (2020).

[38] M Born, K Huang and M Lax *Am. J. Phys,* **23** 474 (1955).

[39] S F Pugh *Lond. Edinb. Dublin Philos. Mag. J. Sci.* **45** 823 (1954).

[40] G Kalpana, B Palanivel, I S Banu and M Rajagopalan *Phys. Rev. B* **56** 3532 (1997).

[41] Z L Lv, H L Cui, H Wang, X H Li and G F Ji *Philos. Mag.* **97** 743 (2017).

[42] M Sauvage *Acta Crystallogr. Sect. B: Struct. Crystallogr. Cryst. Chem.* **30** 2786 (1974).

[43] A H Reshak, Z Charifi and H Baaziz *Physica B: Condens. Matter* **403** 711 (2008).

[44] H Beck *J. Solid State Chem.* **17** 275 (1976).